Commun. Comput. Phys.
doi: 10.4208/cicp.2009.08.203

Vol. 7, No. 2, pp. 235-249
February 2010

Charge Renormalization, Thermodynamics, and Structure of Deionized Colloidal Suspensions

Ben Lu and Alan R. Denton*

Department of Physics, North Dakota State University, Fargo, ND 58108-6050, USA.

Received 20 August 2008; Accepted (in revised version) 5 December 2008

Available online 24 August 2009

Abstract. In charge-stabilized colloidal suspensions, highly charged macroions, dressed by strongly correlated counterions, carry an effective charge that can be substantially reduced (renormalized) from the bare charge. Interactions between dressed macroions are screened by weakly correlated counterions and salt ions. Thermodynamic and structural properties of colloidal suspensions depend sensitively on the magnitudes of both the effective charge and the effective screening constant. Combining a charge renormalization theory of effective electrostatic interactions with Monte Carlo simulations of a one-component model, we compute osmotic pressures and pair distribution functions of deionized colloidal suspensions. This computationally practical approach yields close agreement with corresponding results from large-scale simulations of the primitive model up to modest electrostatic coupling strengths.

PACS: 82.70.Dd, 83.70.Hq, 05.20.Jj, 05.70.-a

Key words: Charged colloids, charge renormalization, effective interactions, structure, Monte Carlo simulation.

1 Introduction

Charge-stabilized colloidal suspensions [1–3] exhibit rich thermodynamic phase behavior and tunable materials properties (e.g., thermal, mechanical, optical, rheological) that are the basis of many industrial and technological applications. Thermally excited (Brownian) motion of nm-μm-sized particles dispersed in a fluid medium drives the self-assembly of ordered phases. Important examples are nanoscale structures [4] and colloidal crystals, whose diverse crystalline symmetries and variable lattice constants can conveniently template photonic band-gap materials [5–7].

*Corresponding author. *Email addresses:* benlu.p@gmail.com (B. Lu), alan.denton@ndsu.edu (A. R. Denton)

Interparticle interactions and correlations determine the distribution of microions (counterions and salt ions) around the colloidal macroions and thereby govern microion-mediated electrostatic interactions between macroions. As explained by the landmark theory of Derjaguin, Landau, Verwey, and Overbeek (DLVO) [8,9], repulsive interactions between like-charged macroions can stabilize a suspension against aggregation induced by van der Waals attractive interactions [10,11]. Equilibrium and dynamical properties of charged colloids depend sensitively on electrostatic interactions, which can be widely tuned by adjusting system parameters: size, charge, and concentration of ion species; pH and dielectric constant of solvent.

A powerful approach to modeling charged colloids is molecular simulation of either the primitive model, which includes all ions explicitly, or all-atom models, which include even individual solvent (e.g., water) molecules. At such microscopic resolution, simulations can potentially yield valuable insights into the thermodynamic, structural, and dynamical properties of real suspensions. Currently available processors and algorithms are limited, however, to relatively small systems and low ion size and charge ratios. Furthermore, simulations of microscopically detailed models do not necessarily elucidate the physical mechanisms underlying complex cooperative behavior.

An alternative to brute-force modeling is simulation of a one-component model, derived by pre-averaging over the microion coordinates to obtain *effective* interactions between macroions, screened by implicitly modeled microions. This coarse-grained strategy finesses the computational challenges that plague more explicit models, but relies on practical and accurate approximations for the effective interactions. A previous simulation study [12] validated the one-component model — implemented with linear-response and mean-field approximations — by direct comparison with pressure data from primitive model simulations at modest electrostatic couplings. The eventual breakdown of the model at higher couplings was attributed to failure of linear-screening approximations to account for nonlinear counterion association near macroions.

A recently proposed charge renormalization theory of effective interactions in charged colloids [13] addresses limitations of linear-screening approximations by incorporating an effective (renormalized) macroion charge into the one-component model. Calculations based on a variational approximation for the free energy indicated the potential of the theory to accurately predict thermodynamic properties of suspensions well into the nonlinear-screening parameter regime. The present paper describes complementary Monte Carlo simulations designed to test predictions for both thermodynamics (osmotic pressure) and structure (pair distribution function) of deionized suspensions of highly charged colloids.

The remainder of the paper is organized as follows. Section 2 first reviews the primitive and effective one-component models of charged colloids. Section 3 outlines the charge renormalization theory, which predicts renormalized system parameters: effective macroion charge, volume fraction, and screening constant. Section 4 describes our Monte Carlo simulations, which take as input the renormalized effective interactions. Section 5 compares our results for the pressure and pair distribution function of deion-

ized suspensions with corresponding data from simulations of the primitive model and with predictions of a variational free energy theory. Excellent agreement is obtained, with minimal computational effort, over ranges of macroion charge, volume fraction, and electrostatic coupling strength. Finally, Section 6 closes with a summary and conclusions.

2 Models

The primitive model idealizes the colloidal macroions as charged hard spheres of monodisperse radius a and bare valence Z_0 (charge $-Z_0e$), the microions as point charges, and the solvent as a continuum of uniform dielectric constant ϵ. We limit present consideration to monovalent microions, for which microion-microion correlations are relatively weak, and further assume index-matching of macroions and solvent, justifying neglect of image charges and polarization effects. At absolute temperature T, a characteristic length scale is the Bjerrum length $\lambda_B = e^2/(\epsilon k_B T)$, defined as the distance between a microion pair at which the electrostatic interaction energy rivals the average thermal energy. In a closed volume V, the suspension comprises N_m macroions and $N_\pm$ positive/negative microions, of which N_c are counterions and N_s are salt ion pairs. Global electroneutrality relates the ion numbers via $N_c = N_+ - N_- = Z_0 N_m$. Alternatively, the suspension may be in Donnan equilibrium (e.g., across a semi-permeable membrane) with an electrolyte reservoir that fixes the salt chemical potential.

While the primitive model has the virtue of explicitly representing all ions, simulations face severe computational challenges posed by long-range Coulomb interparticle interactions and large size and charge asymmetries between ion species. Sophisticated numerical algorithms, such as cluster moves [14, 15] and Ewald or Lekner summation [16, 17], can significantly broaden the range of accessible length and time scales. Nevertheless, currently feasible studies are still limited to relatively small systems and modest asymmetries.

An alternative approach to modeling charged colloids is derived from the Hamiltonian H of the primitive model by formally tracing over the degrees of freedom of the microions (μ) in the partition function of the multi-component mixture:

$$\mathcal{Z} = \langle \langle \exp(-H/k_B T) \rangle_\mu \rangle_m = \langle \exp(-H_{\text{eff}}/k_B T) \rangle_m, \tag{2.1}$$

leaving an explicit trace over only the macroion (m) degrees of freedom. The resulting one-component model (OCM) is governed by an effective Hamiltonian

$$H_{\text{eff}} = E + \frac{1}{2} \sum_{i \neq j=1}^{N_m} v_{\text{eff}}(|\mathbf{r}_i - \mathbf{r}_j|) + \cdots, \tag{2.2}$$

a function of the macroion coordinates $\mathbf{r}_i$, which comprises a one-body volume energy E, an effective macroion-macroion pair potential $v_{\text{eff}}(r)$, and higher-order terms involving sums over effective many-body potentials. The volume energy, although independent

of macroion coordinates, depends on the average densities of macroions and salt ions. The effective pair potential arises from screening of the bare Coulomb potential by the implicitly modeled microions.

The computational benefit of reducing the number of components and the interaction range comes at a cost of increased complexity in the effective interactions. Linear-screening and mean-field approximations, which are justifiable in the case of weakly correlated monovalent microions, yield analytical forms for the volume energy and effective pair potential [18–20]. Moreover, many-body effective interactions are usually weak [21, 22]. The range of validity of the conventional OCM is nevertheless limited by the inevitable onset of nonlinear screening with strengthening macroion-counterion correlations. Previous studies [12,22] establish a parameter threshold $Z_0\lambda_B/a \simeq 7$ — characteristic of highly charged latex particles and ionic surfactant micelles — above which nonlinear effects tend to become significant.

The OCM can be extended to more strongly correlated systems by incorporating physical concepts from charge renormalization theory [23]. Counterions that venture sufficiently close to a highly charged macroion may become thermally "bound" — closely associated with the macroion, if not condensed onto its surface [24,25]. As Fig. 1 depicts, counterions localized within a spherical shell surrounding the macroion may be considered to renormalize the bare macroion valence. The composite "dressed" macroion, comprising a bare macroion and its shell of bound counterions, carries a reduced effective valence $Z \leq Z_0$.

Counterions bind to a macroion at a distance at which the electrostatic energy of attraction is comparable to the average thermal energy per counterion. Denoting by $\phi(r)$ the electrostatic potential at distance r from a macroion center, the width of the association shell δ can be defined via

$$e|\phi(a+\delta)| = Ck_BT, \tag{2.3}$$

where C is a dimensionless parameter of order unity. In general, the reference potential should be chosen as the Donnan (average) potential ϕ_D of the suspension, C then being a function of salt concentration. Counterions within an association shell ($a < r < a+\delta$) are presumed bound by the potential well of the respective macroion, while more distant counterions roam free and screen the dressed macroions. In other studies, a similar thermal criterion has been applied to the electrostatic potential [26–28] and the effective pair potential [29].

3 Theory

The effective interaction theory proposed in ref. [13] combines a charge renormalization theory for the effective macroion charge with a mean-field, linear-response theory of the OCM [18–20]. Here we briefly outline the theory, whose predictions for effective interactions are subsequently used as input to our simulations (Section 4).

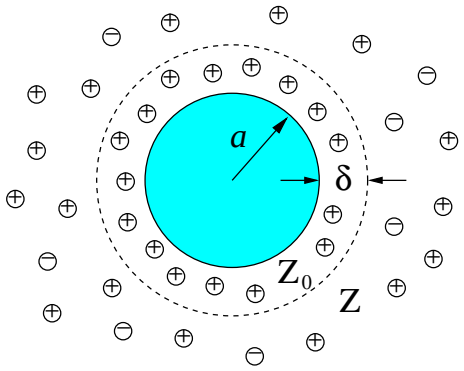

Figure 1: Model of charged colloidal suspension: spherical macroions of radius a and point microions dispersed in a dielectric continuum. Strongly associated counterions in a spherical shell of thickness δ renormalize the bare macroion valence Z_0 to an effective (lower) valence Z.

By invoking a mean-field random-phase approximation for the response functions (partial static structure factors) of a microion plasma, linear-response theory yields analytical expressions for effective electrostatic interactions. This approach proves formally equivalent to density-functional [30–34], extended Debye-Hückel [35], and distribution-function [36, 37] formulations of effective interaction theory [4]. Linear-response theory is also equivalent to linearized Poisson-Boltzmann (PB) theory, based on a consistent linearization of the PB equation and expansion of the ideal-gas free energy functional to quadratic order in the microion density profiles [38].

Linearized theories predict the reduced electrostatic potential generated by a single bare macroion as

$$\psi(r)\equiv\beta\phi(r)=-Z_0\lambda_B\,\frac{e^{\kappa a}}{1+\kappa a}\,\frac{e^{-\kappa r}}{r},\quad r\geq a, \tag{3.1}$$

where $\beta=1/k_BT$, $\kappa=\sqrt{4\pi\lambda_B(n_++n_-)}$ denotes the bare Debye screening constant, and $n_\pm=N_\pm/[V(1-\eta)]$ are the mean number densities of microions in the free volume, i.e., the total volume V reduced by the fraction η occupied by the macroion hard cores. The constraint of global electroneutrality ensures that κ depends implicitly on the average densities of both macroions and salt ions.

Adapting Eq. (3.1) to the charge renormalization model (Fig. 1), the potential around a dressed macroion, of effective valence Z and effective radius $a+\delta$, becomes

$$\tilde{\psi}(r)=-Z\lambda_B\,\frac{e^{\tilde{\kappa}(a+\delta)}}{1+\tilde{\kappa}(a+\delta)}\,\frac{e^{-\tilde{\kappa}r}}{r},\quad r\geq a+\delta, \tag{3.2}$$

where $\tilde{\kappa}=\sqrt{4\pi\lambda_B(\tilde{n}_++\tilde{n}_-)}$ now represents the effective (renormalized) screening constant, $\tilde{n}_\pm=\tilde{N}_\pm/[V(1-\tilde{\eta})]$ and $\tilde{N}_\pm$ are the mean number densities and numbers of free microions, and $\tilde{\eta}=\eta(1+\delta/a)^3$ is the effective volume fraction of the dressed macroions. Combining Eqs. (2.3) and (3.2) yields the transcendental equation

$$\frac{Z\lambda_B}{[1+\tilde{\kappa}(a+\delta)](a+\delta)}=C, \tag{3.3}$$

which may be solved for the association shell thickness δ for given values of Z, η, and C, noting that $\tilde{\kappa}$ depends self-consistently on δ.

The distinction between free and bound microions implies a corresponding separation of the total free energy

$$F = F_{\text{free}} + F_{\text{bound}} + F_m, \tag{3.4}$$

into three terms representing, respectively, contributions from free and bound microions and from macroion effective interactions. The free microions are, by construction, sufficiently weakly correlated with the macroions to be well described by linear-response theory. Their free energy (per macroion) is therefore accurately approximated by the linear-screening prediction for the volume energy (with renormalized parameters):

$$\beta f_{\text{free}} = \sum_{i=\pm} \tilde{x}_i [\ln(\tilde{n}_i \Lambda^3) - 1] - \frac{Z^2}{2} \frac{\tilde{\kappa}\lambda_B}{1+\tilde{\kappa}(a+\delta)} - \frac{Z^2}{2} \frac{n_m}{\tilde{n}_+ + \tilde{n}_-}, \tag{3.5}$$

where $\tilde{x}_\pm = \tilde{N}_\pm / N_m$ are the free microion concentrations, Λ is the microion thermal de Broglie wavelength, and $n_m = N_m/V$ is the mean macroion number density. The three terms on the right side have physical interpretations as the ideal-gas (entropic) free energy of the free microions, the self-energy of the dressed macroions, and the Donnan (average) potential energy of the microions. Although the bound counterions, being relatively strongly correlated with the macroions, do not yield to a linear-response treatment, their free energy (per macroion) can be reasonably approximated by

$$\beta f_{\text{bound}} = (Z_0 - Z) \left[\ln\left(\frac{Z_0 - Z}{v_s} \Lambda^3 \right) - 1 \right] + \frac{Z^2 \lambda_B}{2a}, \tag{3.6}$$

where the first term on the right side is an ideal-gas contribution, $(Z_0 - Z)/v_s$ being the mean counterion density in the association shell of volume $v_s = (4\pi/3)[(a+\delta)^3 - a^3]$, and the second term is the electrostatic energy, assuming tight localization of the counterions near $r = a$.

The effective valence Z is now prescribed, for a given bare valence Z_0, by the variational ansatz [39–41]

$$\left(\frac{\partial}{\partial Z} (f_{\text{free}} + f_{\text{bound}}) \right)_{T, n_\pm} = 0, \tag{3.7}$$

which ensures equality of the chemical potentials of free and bound counterions, under the constraint that Z and δ are connected by Eq. (3.3). The effective valence and shell thickness then determine the effective screening constant $\tilde{\kappa}$.

The macroion free energy F_m in Eq. (3.4) depends on correlations and effective interactions between dressed macroions. Incorporating renormalized system parameters into linear-response theory [19,20], the effective pair potential is given by

$$\beta v_{\text{eff}}(r) = Z^2 \lambda_B \left(\frac{e^{\tilde{\kappa}a}}{1+\tilde{\kappa}a} \right)^2 \frac{e^{-\tilde{\kappa}r}}{r}, \quad r \geq 2(a+\delta), \tag{3.8}$$

whose screened-Coulomb form is identical to the long-range limit of the DLVO pair potential [9]. The renormalized effective interactions and system parameters can be input into computer simulations or liquid-state theories [42] of the OCM to compute thermodynamic and structural properties of bulk suspensions of charged colloids. In the next section, we compare our simulation results with predictions of a variational approximation [22, 30] for the macroion free energy (per macroion) based on first-order thermodynamic perturbation theory with a hard-sphere reference system:

$$f_m(n_m,\tilde{n}_\pm)=\min_{(d)}\left\{f_{\rm HS}(n_m,\tilde{n}_\pm;d)+2\pi n_m\int_d^\infty {\rm d}r^2 g_{\rm HS}(r,n_m;d)\tilde{v}_{\rm eff}(r,n_m,\tilde{n}_\pm)\right\}. \tag{3.9}$$

Here $f_{\rm HS}$ and $g_{\rm HS}$ are, respectively, the excess free energy density and pair distribution function of the HS fluid, computed from the near-exact Carnahan-Starling and Verlet-Weis expressions [42]. Minimization with respect to the effective hard-sphere diameter d yields a least upper bound to the free energy. In practice, the renormalized system parameters (Z, δ, $\tilde{\kappa}$) must be held fixed in this minimization and in all partial thermodynamic derivatives. The corresponding prediction for the thermodynamic pressure is

$$\beta p=n_m+\tilde{n}_++\tilde{n}_--\frac{Z(\tilde{n}_+-\tilde{n}_-)\tilde{\kappa}\lambda_B}{4[1+\tilde{\kappa}(a+\delta)]^2}+n_m^2\beta\left(\frac{\partial f_m}{\partial n_m}\right)_{T,N_s/N_m}, \tag{3.10}$$

where the first three terms on the right side are ideal-gas contributions from macroions and free microions, the fourth term arises from density dependence of the self-energy of the dressed macroions, and the final term is generated by effective interactions between pairs of dressed macroions. While this simple variational theory yields the pressure and other thermodynamic properties, computer simulations or integral-equation theory are required to determine structural properties.

4 Monte Carlo simulations

Working within the canonical (constant-NVT) ensemble, we consider a one-component fluid of macroions in a cubic box, subject to periodic boundary conditions, at fixed temperature, volume, macroion number, and mean salt concentration. The macroions interact with one another via effective electrostatic interactions that depend on the mean densities of both macroions and (implicitly modeled) salt. According to the standard Metropolis algorithm [16, 17], trial particle displacements are accepted with probability

$$P=\min\{\exp(-\beta\Delta U),1\}, \tag{4.1}$$

where $\Delta U=U(n)-U(o)$ is the change in pair potential energy between the new (n) and old (o) states and

$$U=\sum_{i<j=1}^{N_m} v_{\rm eff}(|\mathbf{r}_i-\mathbf{r}_j|) \tag{4.2}$$

is a sum of hard-sphere-repulsive-Yukawa (screened-Coulomb) pair potentials. Note that the acceptance probability for trial displacements does not involve the volume energy, since the mean density is fixed. Consequently, the volume energy does not affect the macroion structure, although it does contribute to the pressure (see below). To achieve high numerical precision, pair interactions were cut off at a distance $r_c \simeq 20/\tilde{\kappa}$, i.e., 20 effective screening lengths. The cut-off radius determined the minimum box side length, $L = 2r_c$, necessary to avoid interactions of a particle with its own periodic images. For a given volume fraction, the requisite number of macroions was therefore prescribed as $N_m \simeq (3\eta/4\pi)(40/\tilde{\kappa}a)^3$.

We performed a series of simulations, using renormalized effective interaction parameters (effective macroion valence, volume fraction, and screening constant), starting from face-centered cubic crystal configurations. Trial moves were executed by randomly displacing macroions with a step size adjusted to yield an acceptance rate of about 50%. Following an equilibration phase of 10^4 cycles, statistics were accumulated for pressures and pair distribution functions over the next 10^4 cycles ($N_m \times 10^4$ particle displacements). Test simulations for larger systems confirmed finite-size effects to be negligible. Relatively modest computing resources were required, with typical runs on a single Intel Xeon-HT processor lasting 30, 120, and 200 hours for $N_m = 2400$, 4000, and 5800 particles, respectively.

In the constant-NVT ensemble, the total pressure may be expressed as

$$\beta p = n_m + \tilde{n}_+ + \tilde{n}_- - \frac{Z(\tilde{n}_+ - \tilde{n}_-)\tilde{\kappa}\lambda_B}{4[1+\tilde{\kappa}(a+\delta)]^2} + \beta p_{\text{pair}}, \tag{4.3}$$

where p_{pair} is generated by effective interactions between pairs of macroions and corresponds to the last term on the right side of Eq. (3.10). The pair pressure is computed from the virial expression for a density-dependent pair potential [43]:

$$p_{\text{pair}} = \left\langle \frac{\mathcal{V}_{\text{int}}}{3V} \right\rangle - \left\langle \left(\frac{\partial U}{\partial V} \right)_{\tilde{N}_s/N_m} \right\rangle + p_{\text{tail}}, \tag{4.4}$$

where $\mathcal{V}_{\text{int}}$ is the internal virial, the volume derivative term accounts for the density dependence of the effective pair potential, angular brackets denote an ensemble average over configurations in the canonical ensemble, and p_{tail} corrects for cutting off the long-range tail of the pair potential. The internal virial is given by

$$\mathcal{V}_{\text{int}} = \sum_{i=1}^{N_m} \mathbf{r}_i \cdot \mathbf{f}_i = \sum_{i<j=1}^{N_m} (1+\tilde{\kappa}r_{ij}) v_{\text{eff}}(r_{ij}), \tag{4.5}$$

where $\mathbf{f}_i = -\sum_{j\neq i} v'_{\text{eff}}(r_{ij})$ is the effective force exerted on macroion i by all neighboring macroions within a sphere of radius r_c. The second term on the right side of Eq. (4.4) is computed as the ensemble average of

$$\left(\frac{\partial U}{\partial V} \right)_{\tilde{N}_s/N_m} = -\frac{n_m}{V} \sum_{i<j=1}^{N_m} \left(\frac{\partial v_{\text{eff}}(r_{ij})}{\partial n_m} \right)_{\tilde{N}_s/N_m} = \frac{1}{V(1-\tilde{\eta})} \sum_{i<j=1}^{N_m} \left(\frac{\tilde{\kappa}r_{ij}}{2} - \frac{\tilde{\kappa}^2 a^2}{1+\tilde{\kappa}a} \right) v_{\text{eff}}(r_{ij}) \,. \tag{4.6}$$

Finally, neglecting pair correlations for $r > r_c$, the tail pressure is approximated by

$$p_{\text{tail}} = -\frac{2\pi}{3} n_m^2 \int_{r_c}^{\infty} \mathrm{d}r r^3 v'_{\text{eff}}(r) = \frac{2\pi}{3} n_m^2 \left(\frac{\tilde{\kappa}^2 r_c^2 + 3\tilde{\kappa} r_c + 3}{\tilde{\kappa}^2} \right) r_c v_{\text{eff}}(r_c) \,. \tag{4.7}$$

The macroion structure of the suspension is characterized by the macroion-macroion pair distribution function $g(r)$, defined such that $4\pi r^2 g(r)\mathrm{d}r$ equals the average number of macroions in a spherical shell of radius r and thickness $\mathrm{d}r$ centered on a macroion. With each particle regarded in turn as the central particle in a given configuration, neighboring particles were assigned to concentric spherical shells (bins), of thickness $\Delta r = 0.1a$, according to their radial distance r from the central particle. Following equilibration, $g(r)$ was computed in the range $2(a+\delta) < r < L/2$ by accumulating statistics of particle numbers in radial bins and averaging over all configurations. The raw distributions were finally smoothed by averaging each bin together with its neighbors in a moving average algorithm.

5 Results and discussion

The renormalized effective interactions (Section 3) previously provided the basis for variational theory calculations of the pressure of deionized suspensions [13]. The same effective interactions are here input into Monte Carlo simulations (Section 4) of the one-component model to compute both the pressure and macroion-macroion pair distribution function. Comparing our results with corresponding data from primitive model simulations allows testing the accuracy of the effective interactions and the variational free energy approximation.

All results presented below are for the case of monovalent counterions, zero salt concentration, and an aqueous solvent at room temperature ($\lambda_B = 0.714$ nm). Throughout, the dimensionless thermal parameter in Eq. (3.3) is fixed at $C = 3$, a value shown in ref. [13] to give satisfactory agreement with pressure data from primitive model simulations. For salt-free suspensions, this choice of C corresponds to

$$e|\phi(a+\delta) - \phi_D| = 2k_B T.$$

In passing, we note that the parameter C is analogous to the adjustable cell radius b in the PB cell theory of Zoetekouw and van Roij [44].

Fig. 2 illustrates the distinction between the bare and effective macroion valences. For a sufficiently small bare valence, Eq. (3.3) has no real-valued solution for any nonzero association shell thickness. In this case, all counterions are free ($\delta = 0$, $v_s = 0$) and the free energy is minimized by $Z = Z_0$. Beyond a threshold bare valence, however, the association shell appears and rapidly thickens with increasing Z_0. Correspondingly, the free energy minimum shifts to $Z < Z_0$. With increasing Z_0, the effective valence grows logarithmically, in contrast to the saturation observed for polyelectrolytes [24, 25] and

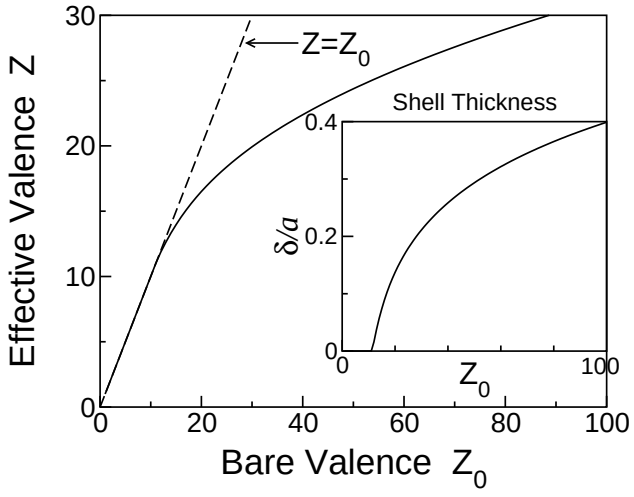

Figure 2: Effective valence Z vs. bare valence Z_0 for a deionized suspension ($c_s \simeq 0$) of macroions of radius $a=2$ nm and volume fraction $\eta=0.01$. Inset: counterion association shell emerges and thickens beyond threshold Z_0.

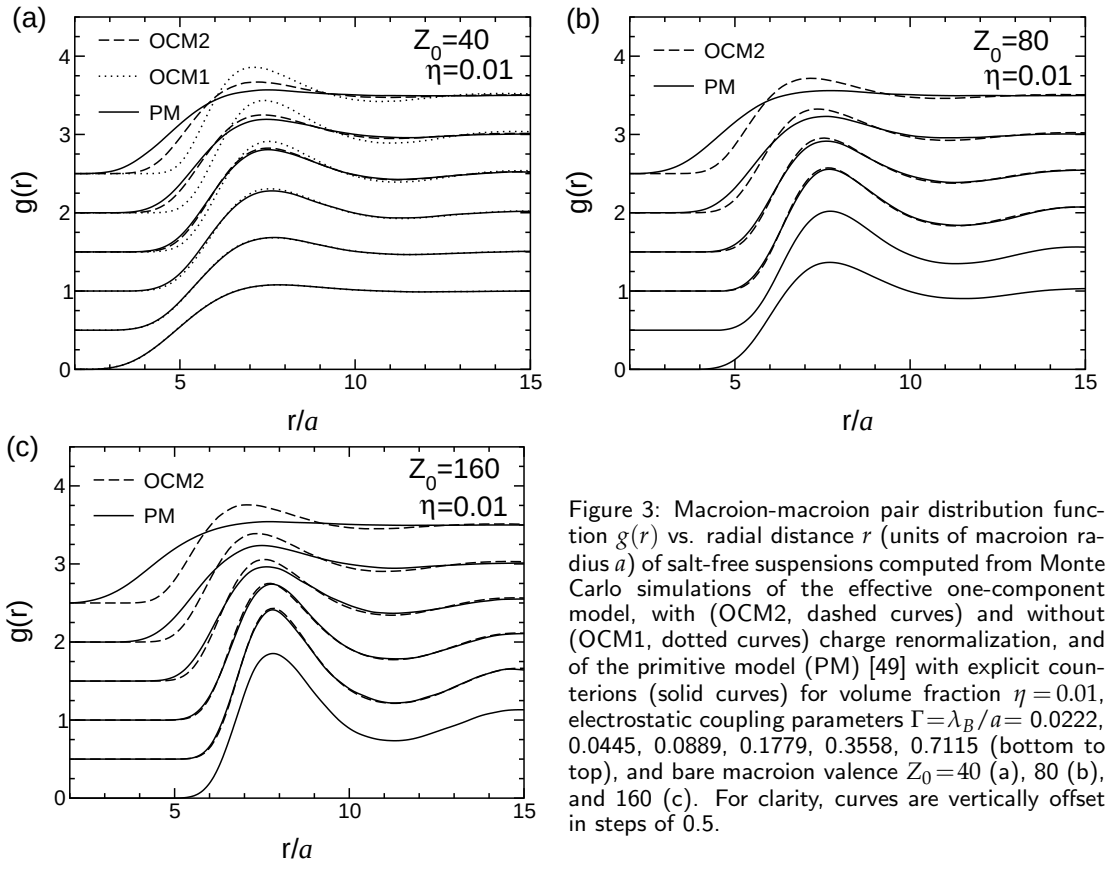

Figure 3: Macroion-macroion pair distribution function $g(r)$ vs. radial distance r (units of macroion radius a) of salt-free suspensions computed from Monte Carlo simulations of the effective one-component model, with (OCM2, dashed curves) and without (OCM1, dotted curves) charge renormalization, and of the primitive model (PM) [49] with explicit counterions (solid curves) for volume fraction $\eta=0.01$, electrostatic coupling parameters $\Gamma=\lambda_B/a=$ 0.0222, 0.0445, 0.0889, 0.1779, 0.3558, 0.7115 (bottom to top), and bare macroion valence $Z_0=40$ (a), 80 (b), and 160 (c). For clarity, curves are vertically offset in steps of 0.5.

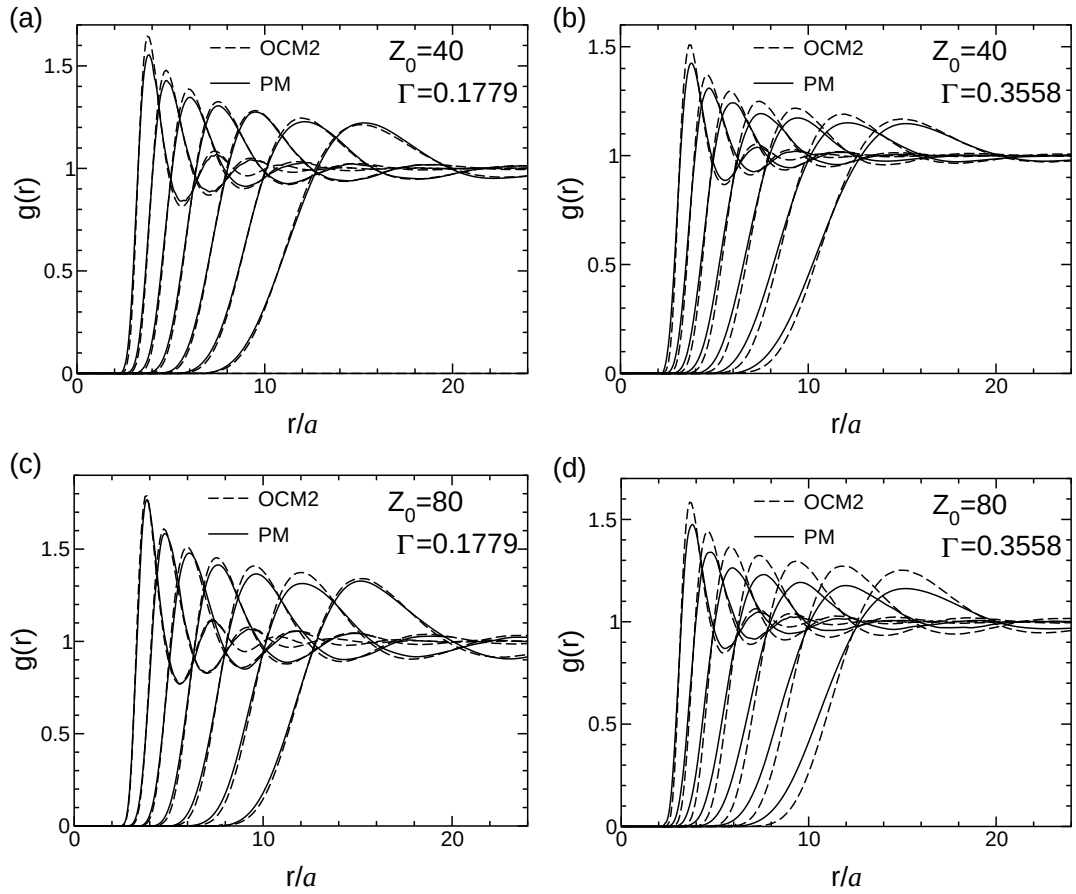

Figure 4: Macroion-macroion pair distribution function $g(r)$ vs. radial distance r (units of macroion radius a) of salt-free suspensions computed from Monte Carlo simulations of the charge-renormalized effective one-component model (OCM2, dashed curves) and of the primitive model [49] (PM, solid curves) for various bare macroion valences Z_0, electrostatic coupling parameters $\Gamma = \lambda_B/a$, and volume fractions $\eta =$ 0.00125, 0.0025, 0.005, 0.01, 0.02, 0.04, and 0.08 (right to left).

predicted for colloidal suspensions by PB cell theories [23, 45, 46] and Debye-Hückel theories [39–41, 47, 48].

We first test the capacity of the charge renormalization theory [13] to predict the macroion structure. Figs. 3 and 4 compare results for the pair distribution function $g(r)$ from our simulations of the OCM, using charge-renormalized effective interactions as input, and corresponding data from extensive Monte Carlo simulations of the primitive model (PM) [49] for salt-free suspensions over ranges of bare valence, volume fraction, and electrostatic coupling strength $\Gamma = \lambda_B/a$. Well beyond the threshold for charge renormalization ($Z_0\Gamma \simeq 7$), the OCM and PM results agree closely. Significant deviations emerge only for $Z_0\Gamma > 15$, the OCM consistently overpredicting the macroion structure. For reference, Fig. 3 also includes OCM results obtained with unrenormalized effective interactions, illustrating the impact of charge renormalization on strongly coupled suspensions.

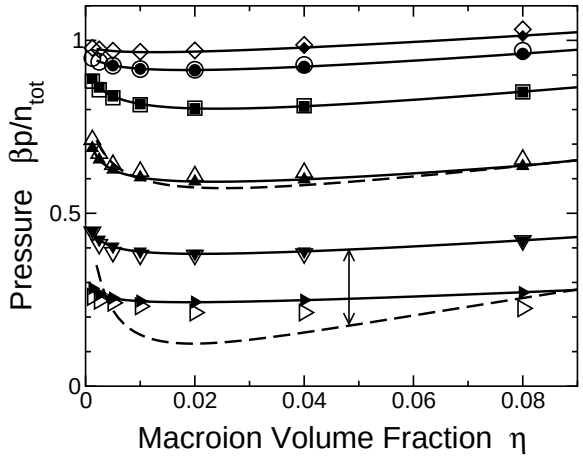

Figure 5: Total reduced pressure $\beta p/n_{\rm tot}$ vs. macroion volume fraction η, where $n_{\rm tot}=(Z_0+1)n_m$ (total ion density), of salt-free suspensions with bare macroion valence $Z_0=40$ and electrostatic coupling constants (from top to bottom) $\Gamma=$ 0.0222, 0.0445, 0.0889, 0.1779, 0.3558, 0.7115. Open symbols: Monte Carlo simulations of the primitive model [49]. Filled symbols: Monte Carlo simulations of the effective one-component model. (Symbol sizes exceed error bars.) Curves: variational theory with (solid) and without (dashed) charge renormalization. The double-ended arrow points to corresponding curves for $\Gamma=0.3558$. The dashed curve for $\Gamma=0.7115$ is off-scale, the pressure being negative.

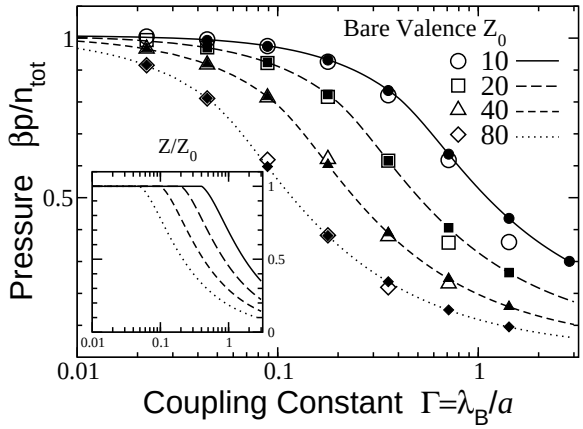

Figure 6: Total reduced pressure $\beta p/n_{\rm tot}$ vs. electrostatic coupling parameter Γ of salt-free suspensions with fixed volume fraction $\eta=0.01$ and bare macroion valence (top to bottom) $Z_0=$ 10, 20, 40, 80. Open symbols: Monte Carlo simulations of the primitive model [49]. Filled symbols: Monte Carlo simulations of the effective one-component model. (Symbol sizes exceed error bars.) Curves: charge-renormalized variational theory. Inset: Ratio of effective to bare macroion valence Z/Z_0 vs. Γ.

Finally, we test predictions of the charge renormalization theory [13] for thermodynamics. Figs. 5 and 6 directly compare the pressures computed from our OCM simulations [via Eqs. (4.3)-(4.7)] with corresponding data from primitive model simulations [49] of salt-free suspensions over ranges of bare valence, volume fraction, and electrostatic coupling strength. The OCM and primitive model results are seen to be in excellent agreement up to the highest couplings for which primitive model data are available

($Z_0\Gamma \simeq 30$), well beyond the charge renormalization threshold. Figs. 5 and 6 also compare the pressures resulting from our OCM simulations with predictions of the variational theory [Eq. (3.10)]. The near exact agreement between simulation and theory for the OCM confirms the accuracy of the variational approximation for the macroion free energy [Eq. (3.9)] and demonstrates the equivalence of the thermodynamic and virial expressions for the pressure, i.e., Eqs. (3.10) and (4.3), respectively.

6 Conclusions

Summarizing, we have performed Monte Carlo simulations of the one-component model of charged colloids, using as input effective electrostatic interactions predicted by a recently proposed charge renormalization theory [13]. Structural and thermodynamic properties of salt-free suspensions are computed and directly compared with simulations of the primitive model. For bare valences Z_0 and electrostatic coupling strengths Γ considerably exceeding the renormalization threshold, the pair distribution function and pressure are in close agreement with corresponding results from simulations of the primitive model. Significant discrepancies between the OCM and PM simulations are observed in $g(r)$ for $Z_0\Gamma > 15$, and in the pressure only for $Z_0\Gamma > 30$. The level of agreement appears to be comparable to the charge-renormalization scheme of ref. [14], which is based on a PB cell model [23]. The computationally practical approach described here may provide a useful modeling alternative, for some applications, to molecular-scale simulations of charged colloids. Further comparisons with primitive model simulation data, particularly at nonzero salt concentrations, would help to chart the validity range of the charge-renormalized OCM.

The threshold for charge renormalization closely coincides with the onset of a spinodal phase instability predicted by linearized effective-interaction theories [22, 30, 32, 35] for deionized (but not salt-free) suspensions of highly charged colloids. Although observations consistent with bulk phase separation have been reported [50–57], the experimental picture of deionized suspensions remains cloudy. Furthermore, the relevant parameter regime is not yet accessible to primitive model simulations. Recent studies based on the PB cell model have concluded that the predicted instability may be an artifact of linearization approximations [58–60]. Preliminary calculations based on the present approach indicate, however, that the phase instability may survive charge renormalization [61]. Future work will continue to explore the remarkable phase behavior of deionized suspensions.

Acknowledgments

This work was supported by the National Science Foundation (DMR-0204020) and the Petroleum Research Fund (PRF 44365-AC7). We thank Per Linse for helpful correspondence and for providing primitive model simulation data.

References

[1] D. F. Evans and H. Wennerström, The Colloidal Domain (2nd ed.) (Wiley-VCH, New York, 1999).
[2] K. S. Schmitz, Macroions in Solution and Colloidal Suspension (VCH, New York, 1993).
[3] P. N. Pusey, in Liquids, Freezing and Glass Transition, session 51, ed. J.-P. Hansen, D. Levesque, and J. Zinn-Justin (North-Holland, Amsterdam, 1991).
[4] A. R. Denton, in Nanostructured Soft Matter: Experiment, Theory, Simulation and Perspectives, ed. A. V. Zvelindovsky (Springer, Dordrecht, 2007).
[5] C. M. Soukoulis, Photonic Band Gap Materials (Kluwer, Dordrecht, 1996).
[6] J. E. G. J. Wijnhoven and W. L. Vos, Science 281, 802 (1998).
[7] J. D. Joannopoulos, Nature 414, 257, (2001); Y. A. Vlasov, X. Z. Bo, J. C. Sturm, and D. J. Norris, Nature 414, 289, (2001).
[8] B. V. Derjaguin and L. Landau, Acta Physicochimica (URSS) 14, 633 (1941).
[9] E. J. W. Verwey and J. T. G. Overbeek, Theory of the Stability of Lyophobic Colloids (Elsevier, Amsterdam, 1948).
[10] J. Israelachvili, Intermolecular and Surface Forces (Academic, London, 1992).
[11] For reviews of colloidal interactions, see C. N. Likos, Phys. Rep. 348, 267 (2001); L. Belloni, J. Phys.: Condens. Matter 12, R549 (2000); J. P. Hansen and H. Löwen, Annu. Rev. Phys. Chem. 51, 209 (2000).
[12] B. Lu and A. R. Denton, Phys. Rev. E 75, 061403 (2007).
[13] A. R. Denton, J. Phys.: Condens. Matter 20, 494230 (2008).
[14] V. Lobaskin and P. Linse, J. Chem. Phys. 111, 4300 (1999).
[15] J. Liu and E. Luijten, Phys. Rev. Lett. 92, 035504 (2004); Phys. Rev. E 71, 066701 (2005).
[16] D. Frenkel and B. Smit, Understanding Molecular Simulation (Academic, London, 2001).
[17] M. P. Allen and D. J. Tildesley, Computer Simulation of Liquids (Oxford, Oxford, 1987).
[18] M. J. Grimson and M. Silbert, Mol. Phys. 74, 397 (1991).
[19] A. R. Denton, J. Phys.: Condens. Matter 11, 10061 (1999).
[20] A. R. Denton, Phys. Rev. E 62, 3855 (2000).
[21] A. R. Denton, Phys. Rev. E 70, 31404 (2004).
[22] A. R. Denton, Phys. Rev. E 73, 41407 (2006).
[23] S. Alexander, P. M. Chaikin, P. Grant, G. J. Morales, and P. Pincus, J. Chem. Phys. 80, 5776 (1984).
[24] G. S. Manning, J. Chem. Phys. 51, 924 (1969).
[25] F. Oosawa, Polyelectrolytes (Dekker, New York, 1971).
[26] K. S. Schmitz, Langmuir 15, 4093 (1999).
[27] V. Sanghiran and K. S. Schmitz, Langmuir 16, 7566 (2000).
[28] A. K. Mukherjee, K. S. Schmitz, and L. B. Bhuiyan, Langmuir 18, 4210 (2002).
[29] D. B. Lukatsky and S. A. Safran, Phys. Rev. E 63, 011405 (2000).
[30] R. van Roij and J.-P. Hansen, Phys. Rev. Lett. 79, 3082 (1997).
[31] H. Graf and H. Löwen, Phys. Rev. E 57, 5744 (1998).
[32] R. van Roij, M. Dijkstra, and J.-P. Hansen, Phys. Rev. E 59, 2010 (1999).
[33] R. van Roij and R. Evans, J. Phys.: Condens. Matter 11, 10047 (1999).
[34] B. Zoetekouw and R. van Roij, Phys. Rev. E 73, 21403 (2006).
[35] P. B. Warren, J. Chem. Phys. 112, 4683 (2000); J. Phys.: Condens. Matter 15, S3467 (2003); Phys. Rev. E 73, 011411 (2006).
[36] B. Beresford-Smith, D. Y. C. Chan, and D. J. Mitchell, J. Coll. Int. Sci. 105, 216 (1985).

[37] D. Y. C. Chan, P. Linse, and S. N. Petris, Langmuir 17, 4202 (2001).
[38] A. R. Denton, Phys. Rev. E 76, 051401 (2007).
[39] Y. Levin, M. C. Barbosa, and M. N. Tamashiro, Europhys. Lett. 41, 123 (1998).
[40] M. N. Tamashiro, Y. Levin, and M. C. Barbosa, Eur. Phys. J. B 1, 337 (1998).
[41] A. Diehl, M. C. Barbosa, and Y. Levin, Europhys. Lett. 53, 86 (2001).
[42] J.-P. Hansen and I. R. McDonald, Theory of Simple Liquids, 2^{nd} edition (Academic, London, 1986).
[43] A. A. Louis, J. Phys.: Condens. Matter 14, 9187 (2002).
[44] B. Zoetekouw and R. van Roij, Phys. Rev. Lett. 97, 258302 (2006).
[45] L. Belloni, Colloids Surf. A 140, 227 (1998).
[46] L. Bocquet, E. Trizac, and M. Aubouy, J. Chem. Phys. 117, 8138 (2002).
[47] Y. Levin, E. Trizac, and L. Bocquet, J. Phys.: Condens. Matter 15, S3523 (2003).
[48] E. Trizac and Y. Levin, Phys. Rev. E 69, 031403 (2004).
[49] P. Linse, J. Chem. Phys. 113, 4359 (2000). Reduced pressures in Table III of this paper should be $\beta p/n_{\rm tot}=0.361$ for $Z=10$, $\Gamma=1.423$, $\eta=0.01$; 0.970 for $Z=40$, $\Gamma=0.0222$, $\eta=0.005$; and 0.971 for $Z=40$, $\Gamma=0.0222$, $\eta=0.02$ (P. Linse, private communication).
[50] B. V. R. Tata, M. Rajalakshmi, and A. K. Arora, Phys. Rev. Lett. 69, 3778 (1992).
[51] K. Ito, H. Yoshida, and N. Ise, Science 263, 66 (1994).
[52] N. Ise and H. Yoshida, Acc. Chem. Res. 29, 3 (1996).
[53] B. V. R. Tata, E. Yamahara, P. V. Rajamani, and N. Ise, Phys. Rev. Lett. 78, 2660 (1997).
[54] N. Ise, T. Konishi, and B. V. R. Tata, Langmuir 15, 4176 (1999).
[55] H. Matsuoka, T. Harada, and H. Yamaoka, Langmuir 10, 4423 (1994); H. Matsuoka, T. Harada, K. Kago, and H. Yamaoka, ibid 12, 5588 (1996); T. Harada, H. Matsuoka, T. Ikeda, and H. Yamaoka, ibid 15, 573 (1999).
[56] A. E. Larsen and D. G. Grier, Nature 385, 230 (1997).
[57] F. Gröhn and M. Antonietti, Macromolecules 33, 5938 (2000).
[58] R. Klein and H. H. von Grünberg, Pure Appl. Chem. 73, 1705 (2001).
[59] M. Deserno and H. H. von Grünberg, Phys. Rev. E 66, 011401 (2002).
[60] M. N. Tamashiro and H. Schiessel, J. Chem. Phys. 119, 1855 (2003).
[61] A. R. Denton, unpublished.